HHS Public Access

Author manuscript

Mater Sci Eng C Mater Biol Appl. Author manuscript; available in PMC 2020 November 01.

Published in final edited form as:

Mater Sci Eng C Mater Biol Appl. 2019 November ; 104: 109905. doi:10.1016/j.msec.2019.109905.

Modulation of biomimetic mineralization of collagen by soluble ectodomain of discoidin domain receptor 2

Arghavan Farzadi[1], **Theodore Renner**[1], **Edward P. Calomeni**[2], **Kayla F. Presley**[3], **Nicole Karn**[4], **John Lannutti**[3], **Lakshmi P. Dasi**[1], **Gunjan Agarwal**[§,1]

[1]Department of Biomedical Engineering, The Ohio State University, Columbus, OH, USA

[2]Renal Pathology, Wexner Medical Center, The Ohio State University, Columbus, OH, USA

[3]Department of Materials Science and Engineering, The Ohio State University, Columbus, OH, USA

[4]Department of Chemistry and Biochemistry, The Ohio State University, Columbus, OH, USA

Abstract

Collagen fibrils serve as the major template for mineral deposits in both biologically derived and engineered tissues. In recent years certain non-collagenous proteins have been elucidated as important players in differentially modulating intra vs. extra-fibrillar mineralization of collagen. We and others have previously shown that the expression of the collagen receptor, discoidin domain receptor 2 (DDR2) positively correlates with matrix mineralization. The objective of this study was to examine if the ectodomain (ECD) of DDR2 modulates intra versus extra-fibrillar mineralization of collagen independent of cell-signaling. For this purpose, a decellularized collagenous substrate, namely glutaraldehyde fixed porcine pericardium (GFPP) was subjected to biomimetic mineralization protocols. GFPP was incubated in modified simulated body fluid (mSBF) or polymer-induced liquid precursor (PILP) solutions in the presence of recombinant DDR2 ECD (DDR2-Fc) to mediate extra or intra-fibrillar mineralization of collagen. Thermogravimetric analysis revealed that DDR2-Fc increased mineral content in GFPP calcified in mSBF while no significant differences were observed in PILP mediated mineralization. Electron microscopy approaches were used to evaluate the quality and quantity mineral deposits. An increase in the matrix to mineral ratio, frequency of particles and size of mineral deposits, was observed in the presence of DDR2-Fc in mSBF. Von Kossa staining and immunohistochemistry analysis of adjacent sections indicated that DDR2-Fc bound to both the matrix and mineral phase of GFPP. Further, DDR2-Fc was found to bind to hydroxyapatite (HAP) particles and enhance the nucleation of mineral deposits in mSBF solutions independent of collagen. Taken together, our observations elucidate DDR2 ECD as a novel player in the modulation of extra-fibrillar mineralization of collagen.

[§]To whom correspondence should be addressed: 288 Bevis Hall, 1080 Carmack Road, Columbus, OH 43210, USA, Phone: 614.292.4213, Fax: 614.247.7799, agarwal.60@osu.edu.

Graphical abstract

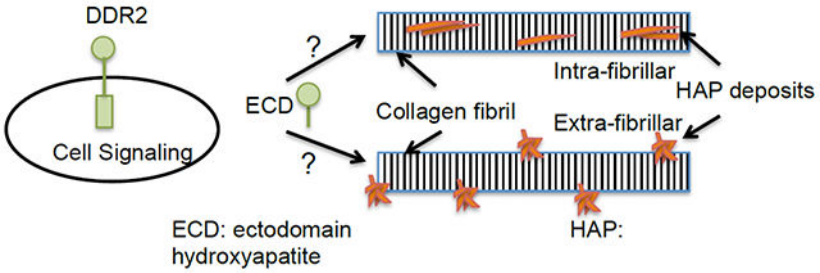

Keywords

collagen; DDR2; hydroxyapatite; mineralization; PILP; SBF

1. Introduction

Extracellular matrix (ECM) mineralization holds widespread relevance for a number of physiological and pathological processes. This includes intra-fibrillar mineralization of collagen fibrils found in lamellar bone[1] and ectopic or extra-fibrillar mineralization of collagen reported in woven bone under physiological conditions and in soft tissues in certain cardiovascular pathologies[2]. In both cases, the mineral deposits comprise largely of calcium phosphate rich hydroxyapatite (HAP). Modulating the mineralization of collagen is thus important for the design and use of biomaterials as implants and scaffolds for bone and cardiovascular tissue engineering. In this regard, mineralization of collagen-rich decellularized animal tissues continue to be of interest because they closely mimic the collagen environment found in-vivo and are commonly employed as bioprosthetic materials[3].

While the chemical and mechanical treatment of bioprosthetic materials is an important parameter in modulating collagen mineralization, growing evidence indicates that, certain matricellular proteins [4] also play an important role. Among these, matricellular proteins are understood to modulate mineralization by interacting with either the mineral phase or with the collagen fibrils in the ECM. For instance fetuin-A[5] and osteopontin[6] are reported to form a stable complex with calcium phosphate in the solution phase, which can then infiltrate into the collagen fibril and initiate intra-fibrillar mineralization of collagen. On the other hand, osteonectin[7], asporin[8], bone sialoprotein and their chimers[9] bind to collagen fibrils and facilitate nucleation, binding or growth of extra-fibrillar HAP crystals. Another set of proteins which are important regulators of ECM mineralization are the ubiquitously expressed collagen receptors, namely integrins ($\alpha_1\beta_1$[10]] and $\alpha_2\beta_1$[11]) and discoidin domain receptors (DDR1[12] and DDR2[13]), which are understood to modulate ECM mineralization primarily by affecting cell differentiation or cell-signaling. It remains to be examined if these collagen receptors also possess the capacity to directly modulate ECM mineralization in a manner similar to matricellular proteins.

In this study, we examined how the soluble ectodomain (ECD) of the collagen receptor, DDR2 modulates biomimetic mineralization of collagen. DDR2 is a receptor tyrosine kinase,[14] which binds to fibrillar collagen(s) including collagen type I. The ECD of DDR2 is both necessary and sufficient for its binding to collagen[15], [16]. The structure of the DDR2 ECD has been elucidated using NMR[17] and X-ray crystallography[18]. Several studies have indicated that DDR2 expression is positively correlated with matrix mineralization. We had previously elucidated that the pre-osteoblast cell-line MC3T3-E1 expressing the soluble or membrane-anchored DDR2-ECD enhanced matrix mineralization[19]. Consistent with these observations, another study revealed that knockdown of full-length DDR2 in osteoblasts suppressed osteogenic marker gene expression and matrix mineralization[20]. *In-vivo*, mice lacking DDR2 have been reported to show delayed mineralization[21]. In SMED patients, an aberrant mineralization has been correlated to missense mutations in DDR2 ECD[22], which result in intracellular confinement of the receptor[23]. However, despite these reports, it is not clear if the DDR2-ECD directly modulates extra or intra-fibrillar mineralization of collagen and if the process is affected by its ability to interact with the collagen or the mineral phase.

To gain insight into the role of DDR2 ECD in modulating collagen mineralization, we employed biomimetic protocols to mediate intra vs. extra-fibrillar mineralization of collagen in the presence vs. absence of soluble recombinant DDR2 ECD. Glutaraldehyde fixed porcine pericardium (GFPP), a naturally derived biomaterial employed in tissue engineering applications[24], [25], was used as a collagenous scaffold. A number of analytical techniques such as Raman spectroscopy, electron microscopy, thermogravimetric analysis (TGA) and histological staining were utilized to analyze the quantity, quality and location of mineral deposits. Biochemical assays were used to evaluate the effect of DDR2-Fc on binding and nucleation of HAP. The results derived from our study elucidate a novel role of the DDR2 ECD in modulating ECM mineralization.

2. Materials and Methods

2.1 Materials:

Glutaraldehyde (0.2%)-fixed porcine pericardium (GFPP) was purchased from Avalon Medical (PERI 11048). Recombinant DDR2-Fc (MW= 190 kD) was purified in-house as described earlier[26]. Briefly, 293T cells were transiently transfected with plasmids encoding DDR2-Fc (ECD of human DDR2 fused to a Fc-tag at the amino terminus) and the conditioned media was collected and utilized for protein purification. Bovine serum albumin (BSA) (MW = 66 kD) was from Fisher Scientific (Hampton, NH). Anti-Fc antibodies were from Jackson ImmunoResearch (West Grove, PA). Horse-radish peroxidase (HRP) and fluorescently conjugated secondary antibodies were purchased from Santa Cruz Biotechnology (Dallas, TX). Hydroxyapatite (HAP) powder was obtained from Sigma Aldrich (St. Louis, MO, USA) and utilized after grinding for 45 min (at amplitude setting of 4) using a Pulverisette 0 Mill (Fritsch GmbH, Idar-Oberstein, Germany). All other chemicals, including poly L-aspartic acid (MW 2000-11000) were from Sigma Aldrich or Fischer Scientific.

2.2 Biomimetic calcification:

In-vitro biomimetic mineralization was carried out using two different protocols: the modified simulated body fluid (mSBF) and polymer-induced liquid-precursor (PILP) protocols to mediate extra and intra-fibrillar mineralization of collagen respectively. The mSBF solution comprised of an aqueous solution with 142 mM Na^+, 5 mM K^+, 1.5 mM Mg^{2+}, 2.5 mM Ca^{2+}, 103 mM Cl^-, 27 mM HCO_3^-, 1 mM HPO_4^{2-}, 0.5 mM SO_4^{2-}, similar to the ionic concentration found in the human blood plasma[27]. The reagents were dissolved in 700 ml of doubly-distilled water (at 37°C) with constant stirring (in the sequence listed in Table 1) and were then added to 100 ml of 75 mM HEPES containing 0.2 M NaOH. The resulting solution was adjusted to a final pH of 7.40 at 36.5°C by titrating with 1.0 M NaOH and then made to a final volume of 1000 ml by adding double-distilled water. The resulting mSBF solution (pH 7.4) was passed through a 0.2 μm membrane filter and stored in the incubator (37°C) for three days to examine the stability of solution[27]. No precipitation was observed, and the mSBF solution remained visibly clear and maintained its pH in this period.

The PILP protocol entailed mixing equal volumes of 9 mM $CaCl_2$ (in Tris buffer, pH 7.4) containing the mineralization inhibitor, poly-L-aspartic acid (50 μg/ml), with 4.2 mM K_2HPO_4 (in Tris buffer pH 7.4). Thereafter, the buffer was passed through a 0.2 μm membrane filter and applied to the samples immediately[28].

Recombinant DDR2-FC proteins (100 μg/ml), were added to mSBF and PILP solutions immediately before use. Segments (~1 cm^2) of the GFPP were rinsed in distilled water and then immersed in the mSBF and PILP solutions (with and without DDR2-Fc) for up to 21 days at 37°C as indicated. The solutions were replenished every 3 to 4 days, and the pH of the solution was monitored every time. Phosphate buffer solution (PBS) (with or without DDR2-Fc)was used as a non-mineralizing control solution. At least n=3 independent experiments were performed for each biomimetic protocol.

2.3 Thermogravimetric analysis (TGA):

TGA was performed using the Q50 TGA instrument (TA Instruments, Delaware) in order to quantify the mineral content in GFPP samples. After biomimetic mineralization protocols, GFPP was washed with distilled water and air-dried at room temperature. The specimens were mounted on a sterilized platinum tray and the initial mass of the sample was determined. Thereafter the samples were heated in an atmosphere of N_2 (50 ml/m in) till the organic material was completely combusted and the residual ash was measured. The heat cycle consisted of a temperature ramp of 20°C per minute till a target temperature of 800°C was achieved. Thereafter the samples were allowed to cool down to room temperature and the final residual ash weight was determined. The remaining mass percent (Wt%) at 800°C were utilized to calculate the mineral to matrix ratio (MMR). Significant differences between MMR across samples was evaluated using an unpaired two-tailed student's t-test. A value of $p<0.05$ was considered to be significantly different.

2.4 Transmission Electron Microscopy (TEM):

Segments (~2 mm) of GFPP were fixed in 4% buffered glutaraldehyde for 24 hours and processed for TEM as previously described[29]. Briefly, after glutaraldehyde fixation and rinsing, the specimens were post fixed in 1% osmium tetroxide. Thereafter, specimens were dehydrated in a graded ethanol series and then embedded in Spurn's epoxy resin (Electron Microscopy Sciences, Fort Washington, PA). Tissue blocks were sectioned with a Leica Ultracut UCT ultramicrotome (Leica Microsystems GmbH, Wein, Austria). Bright field TEM micrographs were generated using a JEOL JEM 1010 TEM (JEOL Ltd. Tokyo, Japan) equipped with a MegaView III digital camera (Olympus Soft Imaging Solutions GmbH, Műnster, Germany). Collagen fibrils and electron-dense mineral deposits in TEM images were analyzed using NIH-ImageJ. All analyses were conducted using TEM micrographs showing longitudinal sections of collagen fibrils by using at least n=3 images from three independent experiments. For ascertaining the mineral-to-matrix ratio (MMR), the TEM micrographs were thresholded to select either the collagen fibrils or the electron-dense mineral deposits. MMR was calculated as the ratio of total area of mineral and collagen content. To quantify the size of mineral deposits, the length of each mineral deposit (n=15) was determined for intra-fibrillar mineralization in PILP samples. In addition, the collagen fibril diameter at the center and end(s) of each mineral deposit was measured to ascertain the percentage change in fibril diameter due to intra-fibrillar mineralization. For extra-fibrillar mineralization in mSBF samples, the number and sizes of particles (mineral deposits) were measured using particle size analysis feature of ImageJ. At least n=300 particles were measured for each sample. Student's unpaired, two-tailed t-test was used to ascertain significant differences in MMR and particle sizes between samples with or without DDR2-Fc. A p-value<0.05 was considered significant.

For analytical TEM analysis, the TEM grids were sputter coated with carbon (3 nm thickness) using Leica ACE600 Coater. The grids were then imaged in dark field using a Tecnai F20 field emission 200 kV TEM/scanning-TEM (STEM) and X-TWIN lens (FEI) equipped with a HAADF (High-Angle Annular Dark Field) capability. Selective area electron diffraction (SAED) was performed on mineral deposits identified in TEM images. Energy dispersive spectroscopy (EDS) was accomplished using an EDAX XLT windowless silicon drift detector (SDD). The resulting EDS spectra were used to generate elemental maps of Ca, P and O and to ascertain the Ca/P ratio from the area under the Ka peaks for Ca and P.

2.5 Raman spectroscopy:

Raman spectroscopy was performed at room temperature on GFPP samples after washing them with distilled water and drying in ambient air. A Renishaw InVia Raman (Gloucestershire UK) spectrometer with an incident wavelength of 785 nm was used to obtain Raman spectra from at least five different spots on each sample. The spectra were collected between400 to 1800 cm^{-1} wavenumber. The Amide III (1242 cm^{-1}), CH_2 deformation (1446 cm^{-1}) and Amide I (1660 cm^{-1}) bands were utilized to represent collagen, while the PO_4^{3-} bands located at ν_1= 955-962 cm^{-1}, ν_2 =430-450 cm^{-1}, and ν_4 = 584–590 cm^{-1} were evaluated to assess mineralization[30], [31]. Spectral intensity was calibrated using the Si-Si characteristic shift at 520 cm^{-1} as an internal standard.

2.6 Histochemical staining:

GFFP specimens were embedded and frozen in OCT (optimal cutting temperature) media, cut into 5 pm thick sections and mounted on polylysine-coated glass slides. Von Kossa staining was used to evaluate the presence of calcific deposits. Briefly, after washing off OCT with copious amounts of water, a 5% (w/v) $AgNO_3$ solution was placed on the sections and incubated for 1 hour in front of a 60-watt lamp. Thereafter the samples were exposed to a 5% sodium thiosulfate solution in water for 5 min, washed and mounted in prolong gold anti-fade mounting media and cover-slipped.

Immunohistochemistry (IHC) of adjacent sections was performed to localize the presence of DDR2-Fc. Briefly, after washing off OCT, the sections were blocked with 2% BSA in PBS solution for 1 hr at room temperature and, thereafter, incubated with anti-Fc primary antibody (1 μg/ml) for 2 hrs at room temperature. The sections were then washed and incubated with HRP-conjugated secondary antibody (1 μg /ml) followed by development with a DAB reagent kit (Vector Laboratories). The samples were mounted and cover-slipped and the slides were imaged using an Olympus IX50 microscope using a 20X objective and a Qcolor 3 color camera.

2.7 Hydroxyapatite binding and nucieation:

Binding of DDR2-FC to HAP was analyzed by incubating 5mg of HAP powder with 200 μl of DDR2-Fc (100 μg/ml) in PBS overnight at 4°C on a turn-table[32]. Thereafter, the samples were centrifuged at 14000 rpm for 10 minutes to sediment the HAP and subjected to an immunostaining protocol. Briefly, the HAP slurry was washed three times in PBS and then incubated with anti-Fc antibody followed by washing and incubation with Alexa 488-conjugated secondary antibody. After final wash steps, an aliquot of the resulting particles was dispersed on a microscope slide, cover slipped and imaged using a Zeiss Axiovert fluorescence microscope.

To monitor if DDR2-Fc modulates the nucleation and growth of HAP independent of collagen, 200 μl of PBS, mSBF or PILP solutions (with or without 100 μg/ml of DDR2-Fc) were incubated in a 96-well microplate at 37°C in a CO_2 incubator with 95% relative humidity[32]. The absorbance of the wells (at 595 nm) was monitored using a microplate reader (Perkin Elmer 2030 reader, Victor X3) for up to 21 days. After 21 days, the supernatant was removed from the wells and the residual mineral deposits in the bottom of wells were retrieved by washing the wells with a 200 μl aliquot of de-ionized water. The resulting wash solutions were spotted on SEM stubs, air dried, gold-coated and imaged using SEM.

3. Results

3.1 Effect of DDR2-Fc on biomimetic mineralization of collagen

To evaluate the effect of DDR2 on the overall quantity of mineralization induced by our biomimetic protocols, we utilized thermogravimetric analysis (TGA). As shown in Figure 1(a), GFPP samples incubated in PILP or mSBF (with or without DDR2-Fc) revealed residual ash weight, indicative of mineral deposits whereas GFPP in the control solution

(PBS) revealed no residual ash weight. The mineral to matrix ration (MMR) was obtained by comparing the residual ash weight at 800°C for various samples (Figure 1b). GFPP incubated in PILP solutions exhibited a significantly higher MMR as compared to that in mSBF (p=0.01). Inclusion of DDR2-Fc in PILP solutions resulted in only a slightly higher MMR as compared to PILP alone, however, the results were not statistically significant (p=0.67, n=3). On the other hand, presence of DDR2-Fc in mSBF solutions, significantly enhanced its MMR with statistical significance (p=0.03, n=3).

We next examined how DDR2-Fc modulates intra vs. extra-fibrillar mineralization of collagen at the sub-micron scale. Towards this end, we examined the location, size and frequency of mineral deposits in bright field TEM images. Collagen fibrils could be clearly identified by their characteristic D-periodicity in bright field TEM images with an average fibril diameter of 64.4 ± 2.8 nm. The electron dense darker regions corresponded to mineral deposits (Figures 2 **and** 3). The elemental composition of the mineral deposits was confirmed using dark-field imaging and energy dispersive spectroscopy (Figure S1–a,b)

GFFP samples incubated in PILP solutions (with/out DDR2-Fc) were characterized with a heterogenous mineral deposition consisting of heavily and sparsely mineralized regions. It was not possible to ascertain the location and size of mineral deposits in heavily mineralized regions. However, sparsely mineralized regions revealed several collagen fibrils consisting of co-linear mineral deposits, characteristic of intrafibrillar mineralization[33] (Figure 2a). As expected for intrafibrillar mineralization, mineralized collagen fibrils (with or without DDR2-Fc) resulted in an increase in the fibril diameter. However, no significant differences in the length of mineral deposits (p=0.23) or increase in fibril diameter (p= 0.94) were observed due to presence of DDR2-Fc (Figure 2b, c).

For samples incubated in mSBF, the mineral distribution was more homogenous and irregular shaped mineral deposits decorating the collagen fibrils could be observed throughout the TEM images (Figure 3a). Quantitative analysis (Figure 3b **and** c) showed an increase in the density of mineral particles as well as a higher population of larger particles in GFPP incubated in mSBF+DDR2-Fc. Thus, taken together, our TGA and TEM analysis indicated that DDR2-Fc enhanced the quantity of extra-fibrillar mineralization of collagen by increasing the number and size of mineral deposits (p=0.02), with no significant effect on intra-fibrillar mineral content.

Raman spectroscopy was employed to evaluate if DDR2 ECD affected the phase and crystallinity of mineral deposits. As shown in Figure 4, Raman spectroscopy could identify the presence of mineralization by the appearance of the major phosphate band at ν_1= 957-962 cm^{-1} as well as the minor bands at ν_2 =430-450 cm^{-1} and ν_4 = 584-590 cm^{-1} in samples incubated in mSBF or PILP solutions. The Raman spectrum of GFPP incubated in PBS indicated the absence of these phosphate bands as Ca^{2+} ions are missing in PBS, and the saline solution could not lead to collagen biomineralization. Interestingly, the amide III and I bands at 1242-1273 cm^{-1} and 1653-1670 cm^{-1} and the CH_2 deformation at 1441-1462 cm^{-1} corresponding to collagen could be clearly observed in GFPP samples incubated in PBS and PILP but were not easily discernable in mSBF samples. These observations were consistent with the extra-fibrillar location of mineral deposits in mSBF samples where the

mineral deposits are not expected to be completely co-incident with the contour of the collagen fibrils. Analysis of the major phosphate band (ν_1) revealed that DDR2-Fc did not affect the central location of the major phosphate band in either mSBF or PILP-incubated samples ($p>0.20$), indicating little effect on the quality of the mineral phase [34]. However, the presence of DDR2-Fc led to a decrease in the full-width at half maxima (FWHM) of the major phosphate band in mSBF-incubated samples ($p= 0.001$) indicative of transformation to highly crystalline apatite, (Figure 4b)[35]. The FWHM of PILP incubated samples showed no significant differences in the presence vs. absence of DDR2-Fc ($p=0.34$). To further analyze the effect of DDR2-Fc in modulating the crystallinity of mineral deposits we examined selected area electron diffraction (SAED) pattern arising from mineral deposits in TEM images. As shown in (Figure 4c), SAED of mineral deposits in mSBF samples showed a diffuse pattern (characteristic of poor crystallinity) whereas those in mSBF+DDR2 revealed discrete ring-like pattern (characteristic of crystalline structure). SAED of mineral deposits in PILP samples also revealed discrete rings both in the presence and. absence of DDR2. Our SAED results were thus consistent with Raman spectroscopy analysis and indicated that DDR2-Fc enhanced the crystallinity of the mineral deposits in mSBF samples.

3.2 Interaction of DDR2-Fc with the matrix and mineral phase

Since DDR2-Fc is a collagen-binding protein, we next evaluated if modulation of collagen mineralization by DDR2-ECD was dependent on its binding to the collagen and/or the mineral phase of GFPP by employing histochemical stains like Von Kossa (VK) staining and immunohistochemistry (IHC) (using anti-Fc antibodies) on adjacent sections. Figure 5 shows light microscopy images of VK and IHC staining of GFPP incubated in PBS, mSBF or PILP containing 100 μg /ml DDR2-Fc as indicated. VK staining could identify the presence of calcific deposits on all samples incubated in PILP (Figure 5 e, g) or mSBF (Figure 5 I, k) solutions, but not in the non-mineralizing PBS control (Figure a, c). IHC yielded a positive signal when GFPP (in non-mineralizing PBS buffer) was incubated with recombinant DDR2-Fc (Figure 5d), thus indicating binding of DDR2-Fc to GFPP even before mineralization. Our IHC results also showed a positive signal when DDR2-Fc was present in the solution phase i.e. in PILP (Figure 5h) or mSBF (Figure 5l) thus indicating that DDR2-FC could bind to GFPP during the mineralization process. Similar staining was observed when sections of GFPP pre-incubated in mSBF or PILP (without DDR2-Fc) were post-incubated with DDR2-Fc in PBS for 24 hrs (insets in Figure 5f, j). Thus, our investigations revealed that DDR2-Fc could bind to the collagenous GFPP before, during and after bio-mimetically induced mineralization.

To examine if DDR2-Fc directly interacts with HAP independent of collagen, we carried out a binding assay by incubating DDR2-Fc solutions with a slurry of HAP powder in PBS. Immunostaining of HAP particles confirmed the presence of DDR2-Fc whereas no specific signal was detected using anti-Fc antibodies when a control protein (BSA) was used (Figure 6). We next examined if DDR2-Fc affected the nucleation process of HAP in biomimetic solutions independent of collagen. As shown in Figure 7, the presence of DDR2-Fc resulted in a rise in absorbance as early as 3 days after incubation in mSBF solution whereas PBS and PILP solutions maintained a nearly constant absorbance. SEM analysis of the material deposited in the wells after 21 days revealed spherical-shaped mineral particles characteristic

of HAP. These mineral particles were abundant in mSBF and PILP solutions containing DDR2-Fc but were rarely visible in solutions devoid of DDR2-Fc (data not shown). The particle size was significantly larger for mSBF+DDR2-Fc samples than that observed for PILP+DDR2-Fc, consistent with its earlier rise in turbidity. Thus, taken together, the ability of DDR2-Fc to bind to collagen and HAP as well as to promote nucleation of HAP was consistent with its ability to enhance extrafibrillar mineralization of the collagenous GFPP.

4. Discussion

Previous studies on biomimetic mineralization of collagen have primarily used in-vitro reconstituted collagenous substrates comprising of collagen sponges[6], films[36] or lyophilized collagen. Limited studies exist on biomimetic mineralization of naturally derived biogenic collagen scaffold such as demineralized bone[37], tendons[38] and decellularized heart valve leaflets[39]. In this study we used GFPP as a collagenous substrate as it represents a commonly used bioprosthetic material and closely mimics the native collagen environment found in-vivo. Our studies on GFPP thus hold particular relevance for soft-tissue mineralization as found in cardiovascular pathologies and to understand how processes like cell adhesion and migration can be affected by mineralized collagen[40].

We employed biomimetic mineralization using PILP and mSBF solutions to specifically induce intra and extra-fibrillar mineralization of collagen respectively. As shown in previous studies, the PILP solution includes poly-L-aspartic acid (PAsp) which inhibits mineralization in the solution phase and promotes the diffusion of mineral-PAsp complexes into the collagen fibril[41]. In this case, the mineral starts growing along the nanoscale channels in the collagen fibrils resulting in intra-fibrillar mineralization along the fibril axis[42] as observed in our TEM images. The mSBF solution has been shown to induce bio-mimetic mineralization of collagen as well as other substrates[43]. In this case the collagen fibril serves as a precursor to nucleate hydroxyapatite formation on its surface and thereby induce mineral growth[44]. Such a mineral growth is similar to that induced by seeding SBF or mSBF solutions with hydroxyapatite particles[45]. Since the mineral growth in this case occurs on the fibril surface, it is not constrained by the fibril geometry and the crystals grow in different directions generating spheroid-like structures as seen in our TEM images. Thus both the location as well as the micro-morphology of mineral deposits are a distinguishing feature of intra- versus extra-fibrillar mineralization of collagen and can be achieved biomimetically by usingt PILP or mSBF solutions respectively.

We show that the ectodomain of DDR2 enhances extra-fibrillar mineralization of collagen in GFPP with little impact on intra-fibrillar mineralization. This enhancement of extra-fibrillar mineralization by DDR2-ECD can be attributed to its collagen-binding ability as well as its capacity to bind to and nucleate HAP. While binding of DDR2 to monomeric collagen and collagen-mimetic peptides has previously been elucidated by us[46] and others[47], much less is understood about the ability of DDR2 to bind to collagen fibrils[48]. Our results show that DDR2 ECD may also bind to collagen fibrils which are the primary component of GFPP used in this study. These observations are consistent with a recent study which reports that recombinant DDR2-Fc did bind to collagen fibrils, though the cross-linking of collagen by carbodiimide attenuated its binding[49]. It should be noted that collagen fibrils in the

GFPP are subjected to glutaraldehyde mediated cross-linking which may have impacted DDR2-binding and or PILP-mediated mineralization[36].

Our results reveal an unexpected and novel role of DDR2 ECD in binding to and promoting nucleation and growth of HAP. While the increased frequency of extra-fibrillar mineral deposits observed in samples containing DDR2-Fc may in part be due to its ability to bind to collagen fibrils, the increase in size of extra-fibrillar mineral deposits can be explained by the ability of DDR2-Fc to nucleate HAP, both these processes contributing to an increase in MMR. Another interesting feature observed in our studies was that DDR2-Fc enhanced the crystallinity of extra-fibrillar mineral deposits formed in mSBF solutions. This can also be partly explained by the faster growth rate of mineral deposits observed in the presence of DDR2-Fc. Further studies are required to determine which sites in the DDR2 ECD are responsible for its binding to HAP and whether the full-length cell-surface bound receptor is capable of similar effects. Binding of NCPs to HAP is reported to be mediated by clusters of negatively charged amino acids (e.g. aspartic acid, glutamic acid and phosphoserines)[50], glucosaminoglycans (GAG) chains[51] and/or their affinity for calcium. The DDR2 ECD does consist of several acidic residues as well as putative serine phosphorylation sites which would need to be characterized to understand the molecular mechanism behind its HAP binding property.

Interestingly, no significant effect of DDR2-ECD was observed on intra-fibrillar mineralization of collagen. In our studies, poly aspartic acid (PAsp) in the PILP solution was utilized as a polyanion, which inhibits mineralization in solution and mediates the diffusion of mineral-PAsp complexes into the collagen fibrils[52]. To examine if DDR2-Fc had a similar role as PAsp, we also conducted experiments that replaced PAsp with DDR2-Fc in PILP solutions. However, these solutions resulted in extra-fibrillar mineralization of collagen with no indication of intra-fibrillar mineral deposits (Figure S2 in supporting information). Further, in the absence of the collagenous substrate, DDR2-Fc could promote mineralization in PILP solutions albeit after a longer delay and to a much lesser extent than that in mSBF solution. Thus, taken together, DDR2 ECD acts in a manner opposite to that of NCPs like fetuin[5] and ostepontin[53] by promoting mineralization in the solution phase resulting in enhanced ectopic or extra-fibrillar mineralization of collagen.

5. Conclusion

Our results show that the ectodomain of the collagen receptor DDR2 is a promoter of mineralization in the solution phase and results in enhanced extra-fibrillar mineralization of collagen. It is thus likely that the full-length DDR2 present in cells may act in a similar manner. Our results that DDR2 ECD can promote nucleation of HAP independent of collagen suggest that DDR2 could promote mineralization on even non-collagenous materials. DDR2 ECD can thus be employed to enhance biomimetic mineralization of engineered tissues. On the other hand, inhibition of DDR2 ECD may thus serve as a therapeutic avenue for attenuating ectopic mineralization in cardiovascular pathologies. Taken together, we elucidate DDR2 ectodomain as a novel player in directly modulating extra-fibrillar mineralization of collagenous tissue independent of cell signaling.

Supplementary Material

Refer to Web version on PubMed Central for supplementary material.

Acknowledgement

This work was supported in part by NSF CMMI award 1201111 to GA and a facility grant from the Institute of Materials Research at OSU. We acknowledge Henk Colijn at CEMAS facility at OSU for assistance in obtaining SAED images.

References

[1]. W. T Liu Y, Luo D, "Hierarchical Structures of Bone and Bioinspired Bone Tissue Engineering," Small, vol. 12, no. 34, pp. 4611–32, 2016. [PubMed: 27322951]

[2]. Reznikov N, Steele JAM, Fratzl P, and Stevens MM, "A materials science vision of extracellular matrix mineralization," Nat. Rev. Mater, vol. 1, pp. 1–14, 2016.

[3]. Schmidt CE and Baier JM, "Acellular vascular tissues: Natural biomaterials for tissue repair and tissue engineering," Biomaterials, vol. 21, no. 22 pp. 2215–2231, 2000. [PubMed: 11026628]

[4]. Gorski JP, "Biomineralization of bone: a fresh view of the roles of non-collagenous proteins.," Front. Biosci. (Landmark Ed, vol. 16, pp. 2598–621, 1 2011. [PubMed: 21622198]

[5]. Price PA, Toroian D, and Lim JE, "Mineralization by inhibitor exclusion. The calcification of collagen with fetuin," J. Biol. Chem, vol. 284, no. 25, pp. 17092–17101, 2009. [PubMed: 19414589]

[6]. Rodriguez DE et al., "Multifunctional role of osteopontin in directing intrafibrillar mineralization of collagen and activation of osteoclasts.," Acta Biomater, vol. 10, no. 1, pp. 494–507, 1 2014. [PubMed: 24140612]

[7]. Termine JD, Kleinman HK, Whitson SW, Conn KM, McGarvey ML, and Martin GR, "Osteonectin, a bone-specific protein linking mineral to collagen," Cell, vol. 26, no. 1 PART 1, pp. 99–105, 1981. [PubMed: 7034958]

[8]. Kalamajski S, Aspberg A, Lindblom K, Heinegard D, and Oldberg A, "Asporin competes with decorin for collagen binding, binds calcium and promotes osteoblast collagen mineralization," Biochem. J, vol. 423, no. 1, pp. 53–59, 2009. [PubMed: 19589127]

[9]. Hunter GK, Poitras MS, Underhill TM, Grynpas MD, and Goldberg HA, "Induction of collagen mineralization by a bone sialoprotein-decorin chimeric protein," J. Biomed. Mater. Res, vol. 55, no. 4, pp. 496–502, 2001. [PubMed: 11288077]

[10]. Olivares-Navarrete R et al., "Role of integrin subunits in mesenchymal stem cell differentiation and osteoblast maturation on graphitic carbon-coated microstructured surfaces," Biomaterials, vol. 51, pp. 69–79, 2015. [PubMed: 25770999]

[11]. Jikko A, Harris SE, Chen D, Mendrick DL, and Damsky CH, "Collagen integrin receptors regulate early osteoblast differentiation induced by BMP-2," J. Bone Miner. Res, vol. 14, no. 7, pp. 1075–1083, 1999. [PubMed: 10404007]

[12]. Ahmad PJ et al., "Discoidin domain receptor-1 deficiency attenuates atherosclerotic calcification and smooth muscle cell-mediated mineralization.," Am. J. Pathol, vol. 175, no. 6, pp. 2686–96, 12 2009. [PubMed: 19893047]

[13]. Ge C et al., "Discoidin Receptor2 Controls Bone Formation and Marrow Adipogenesis," J. Bone Miner. Res, vol. 31, no. 12, pp. 2193–2203, 2016. [PubMed: 27341689]

[14]. Fu H-L et al., "Discoidin domain receptors: Unique receptor tyrosine kinases in collagen-mediated signaling," J. Biol. Chem, vol. 288, no. 11,2013.

[15]. Shrivastava A et al., "An Orphan Receptor Tyrosine Kinase Family Whose Members Serve as Nonintegrin Collagen Receptors," Mol. Cell, vol. 1, no. 1, pp. 25–34, 12 1997. [PubMed: 9659900]

[16]. Vogel W, Gish GD, Alves F, and Pawson T, "The Discoidin Domain Receptor Tyrosine Kinases Are Activated by Collagen," Mol. Cell, vol. 1, no. 1, pp. 13–23, 12 1997. [PubMed: 9659899]

[17]. Ichikawa O, Osawa M, Nishida N, Goshima N, Nomura N, and Shimada I, “Structural basis of the collagen-binding mode of discoidin domain receptor2,” EMBO J, vol. 26, no. 18, pp. 4168–4176, 2007. [PubMed: 17703188]

[18]. Carafoli F et al., “Crystallographic insight into collagen recognition by discoidin domain receptor 2.,” Structure, vol. 17, no. 12, pp. 1573–81, 12 2009. [PubMed: 20004161]

[19]. Flynn LA, Blissett AR, Calomeni EP, and Agarwal G, “Inhibition of collagen fibrillogenesis by cells expressing soluble extracellular domains of DDR1 and DDR2,” J Mol Biol, vol. 395, no. 3, pp. 533–543, 2009. [PubMed: 19900459]

[20]. Lin K-L, Chou C-H, Hsieh S-C, Hwa S-Y, Lee M-T, and Wang F-F, “Transcriptional upregulation of DDR2 by ATF4 facilitates osteoblastic differentiation through p38 MAPK-mediated Runx2 activation.,” J. Bone Miner. Res, vol. 25, no. 11, pp. 2489–503, 11 2010. [PubMed: 20564243]

[21]. Ge C, Mohamed F, Binrayes A, Kapila S, and Franceschi RT, “Selective Role of Discoidin Domain Receptor 2 in Murine Temporomandibular Joint Development and Aging,” J. Dent. Res, vol. 97, no. 3, pp. 321–328, 2018. [PubMed: 29073363]

[22]. Bargal R et al., “Mutations in DDR2 Gene Cause SMED with Short Limbs and Abnormal Calcifications,” Am. J. Hum. Genet, vol. 84, no. 1, pp. 80–84, 2009. [PubMed: 19110212]

[23]. Al-Kindi A et al., “A novel mutation in DDR2 causing spondylo-meta-epiphyseal dysplasia with short limbs and abnormal calcifications (SMED-SL) results in defective intra-cellular trafficking.,” BMC Med. Genet, vol. 15, p. 42, 1 2014. [PubMed: 24725993]

[24]. Badylak SF, Freytes DO, and Gilbert TW, “Extracellular matrix as a biological scaff old material: Structure and function,” Acta Biomater, vol. 5, no. 1, pp. 1–13, 2009. [PubMed: 18938117]

[25]. Schoen FJ, Tsao JW, and Levy RJ, “Calcification of bovine pericardium used in cardiac valve bioprostheses. Implications for the mechanisms of bioprosthetic tissue mineralization.,” Am. J. Pathol, vol. 123, no. 1, pp. 134–45, 1986. [PubMed: 2421577]

[26]. Yeung D et al., “Clustering, Spatial Distribution, and Phosphorylation of Discoidin Domain Receptors 1 and 2 in Response to Soluble Collagen I,” J. Mol. Biol, vol. 431, no. 2, pp. 368–390, 2019. [PubMed: 30458172]

[27]. Oyane A, Onuma K, Ito A, Kim H-M, Kokubo T, and Nakamura T, “Formation and growth of clusters in conventional and new kinds of simulated body fluids.,” J. Biomed. Mater. Res. A, vol. 64, pp. 339–348, 2003. [PubMed: 12522821]

[28]. Li Y and Aparicio C, “Discerning the subfibrillar structure of mineralized collagen fibrils: a model for the ultrastructure of bone.,” PLoSOne, vol. 8, no. 9, p. e76782, 1 2013.

[29]. Tonniges JR et al., “Collagen Fibril Ultrastructure in Mice Lacking Discoidin Domain Receptor 1.,” Microsc. Microanai, vol. 22, no. 3, pp. 599–611, 6 2016.

[30]. Mandair FS and Morris MD, “Contributions of Raman spectroscopy to the understanding of bone strength,” Bonekey Rep, vol. 4, 2015.

[31]. Gullekson C, Lucas L, Hewitt K, and Kreplak L, “Surface-sensitive Raman spectroscopy of collagen I fibrils,” Biophys. J, vol. 100, no. 7, pp. 1837–1845, 2011. [PubMed: 21463598]

[32]. Abbarin N, San Miguel S, Holcroft J, Iwasaki K, and Ganss B, “The enamel protein amelotin is a promoter of hydroxyapatite mineralization,” J. Bone Miner. Res, vol. 30, no. 5, pp. 775–785, 2015. [PubMed: 25407797]

[33]. Liu Y et al., “Intrafibrillar collagen mineralization produced by biomimetic hierarchical nanoapatite assembly,” Adv. Mater, vol. 23, no. 8, pp. 975–980, 2011. [PubMed: 21341310]

[34]. Stammeier JA, Purgstaller B, Hippier D, Mavromatis V, and Dietzel M, “ln-situ Raman spectroscopy of amorphous calcium phosphate to crystalline hydroxyapatite transformation,” MethodsX, vol. 5, pp. 1241–1250, 2018. [PubMed: 30364715]

[35]. Gajjeraman S, Narayanan K, Hao J, Qin C, and George A, “Matrix macromolecules in hard tissues control the nucleation and hierarchical assembly of hydroxyapatite,” J. Biol. Chem, vol. 282, no. 2, pp. 1193–1204, 2007. [PubMed: 17052984]

[36]. Li Y et al., “Biomimetic mineralization of woven bone-like nanocomposites: role of collagen cross-links.,” Biomacromolecules, vol. 13, no. 1, pp. 49–59, 1 2012. [PubMed: 22133238]

[37]. Thula TT, Rodriguez DE, Lee MH, Pendi L, Podschun J, and Gower LB, “In vitro mineralization of dense collagen substrates: a biomimetic approach toward the development of bone-graft materials.,” Acta Biomater, vol. 7, no. 8, pp. 3158–69, 8 2011. [PubMed: 21550424]

[38]. Saxena N et al., “Influence of fluoride on the mineralization of collagen via the polymer-induced liquid-precursor (PILP) process,” Dent. Mater, vol. 34, no. 9, pp. 1378–1390, 2018. [PubMed: 29935767]

[39]. Zhai W, Chang J, Lü X, and Wang Z, “Procyanidins-crosslinked heart valve matrix: Anticalcification effect,” J. Biomed. Mater. Res. - Part B Appi. Biomater, vol. 90 B, no. 2, pp. 913–921, 2009.

[40]. Song YH, Friedrichs J, Choi S, Werner C, Estroff LA, and Fischbach C, “Intrafibrillar, bone-mimetic collagen mineralization regulates breast cancer cell adhesion and migration,” Biomaterials, 2018.

[41]. Nudelman F et al., “The role of collagen in bone apatite formation in the presence of hydroxyapatite nucleation inhibitors.,” Nat. Mater, vol. 9, no. 12, pp. 1004–9, 12 2010. [PubMed: 20972429]

[42]. Jee S-S, Thula TT, and Gower LB, “Development of bone-like composites via the polymer-induced liquid-precursor (PILP) process. Part 1: Influence of polymer molecular weight,” Acta Biomater, vol. 6, no. 9, pp. 3676–3686, 9 2010. [PubMed: 20359554]

[43]. Ikeda Y, Neshatian M, Holcroft J, and Ganss B, “The enamel protein ODAM promotes mineralization in a collagen matrix,” Connect. Tissue Res, 2018.

[44]. Liu Y et al., “Hierarchical and non-hierarchical mineralisation of collagen,” Biomaterials, 2011.

[45]. Spanos N, Misirlis DY, Kanellopoulou DG, and Koutsoukos PG, “Seeded growth of hydroxyapatite in simulated body fluid,” J. Mater. Sci, 2006.

[46]. Agarwal G, Kovac L, Radziejewski C, and Samuelsson SJ, “Binding of discoidin domain receptor 2 to collagen I: an atomic force microscopy investigation.,” Biochemistry, vol. 41, no. 37, pp. 11091–11098, 2002. [PubMed: 12220173]

[47]. Konitsiotis AD, Raynal N, Bihan D, Hohenester E, Farndale RW, and Leitinger B, “Characterization of high affinity binding motifs for the discoidin domain receptor DDR2 in collagen.,” J. Biol. Chem, vol. 283, no. 11, pp. 6861–8, 3 2008. [PubMed: 18201965]

[48]. Bhadriraju K, Chung K-H, Spurlin TA, Haynes RJ, Elliott JT, and Plant AL, “The relative roles of collagen adhesive receptor DDR2 activation and matrix stiffness on the downregulation of focal adhesion kinase in vascular smooth muscle cells.,” Biomaterials, vol. 30, no. 35, pp. 6687–94, 12 2009. [PubMed: 19762078]

[49]. Malcor JD et al., “Coupling of a specific photoreactive triple-helical peptide to crosslinked collagen films restores binding and activation of DDR2 and VWF,” Biomaterials, vol. 182, pp. 21–34, 2018. [PubMed: 30099278]

[50]. Milan AM, Sugars RV, Embery G, and Waddington RJ, “Adsorption and interactions of dentine phosphoprotein with hydroxyapatite and collagen,” Eur. J. Oral Sci, vol. 114, no. 3, pp. 223–231, 2006. [PubMed: 16776772]

[51]. Sugars RV, Milan AM, Brown JO, Waddington RJ, Hall RC, and Embery G, “Molecular interaction of recombinant decorin and biglycan with type I collagen influences crystal growth,” Connect. Tissue Res, vol. 44Suppl 1, pp. 189–195, 2003. [PubMed: 12952196]

[52]. Cantaert B, Beniash E, and Meldrum FC, “The role of poly(aspartic acid) in the precipitation of calcium phosphate in confinement,” J. Mater. Chem. B, vol. 1, no. 48, pp. 6586–6595, 2013.

[53]. Steitz SA et al., “Osteopontin inhibits mineral deposition and promotes regression of ectopic calcification,” Am. J. Pathol, vol. 161, no. 6, pp. 2035–2046, 2002. [PubMed: 12466120]

Highlights

- Ectodomain of the collagen receptor, discoidin domain receptor 2 (DDR2-ECD) was examined for its ability to mineralize collagen in biomimetic protocols.
- DDR2-ECD enhanced extrafibrillar mineralization of collagen with little effect on intrafibrillar mineralization in decellularized pericardium tissue.
- DDR2-ECD promoted nucleation and growth of hydroxyapatite independent of collagen.
- DDR2 ECD could be of relevance in modulating biomimetic mineralization of engineered tissues or to understand ectopic mineralization in cardiovascular pathologies.

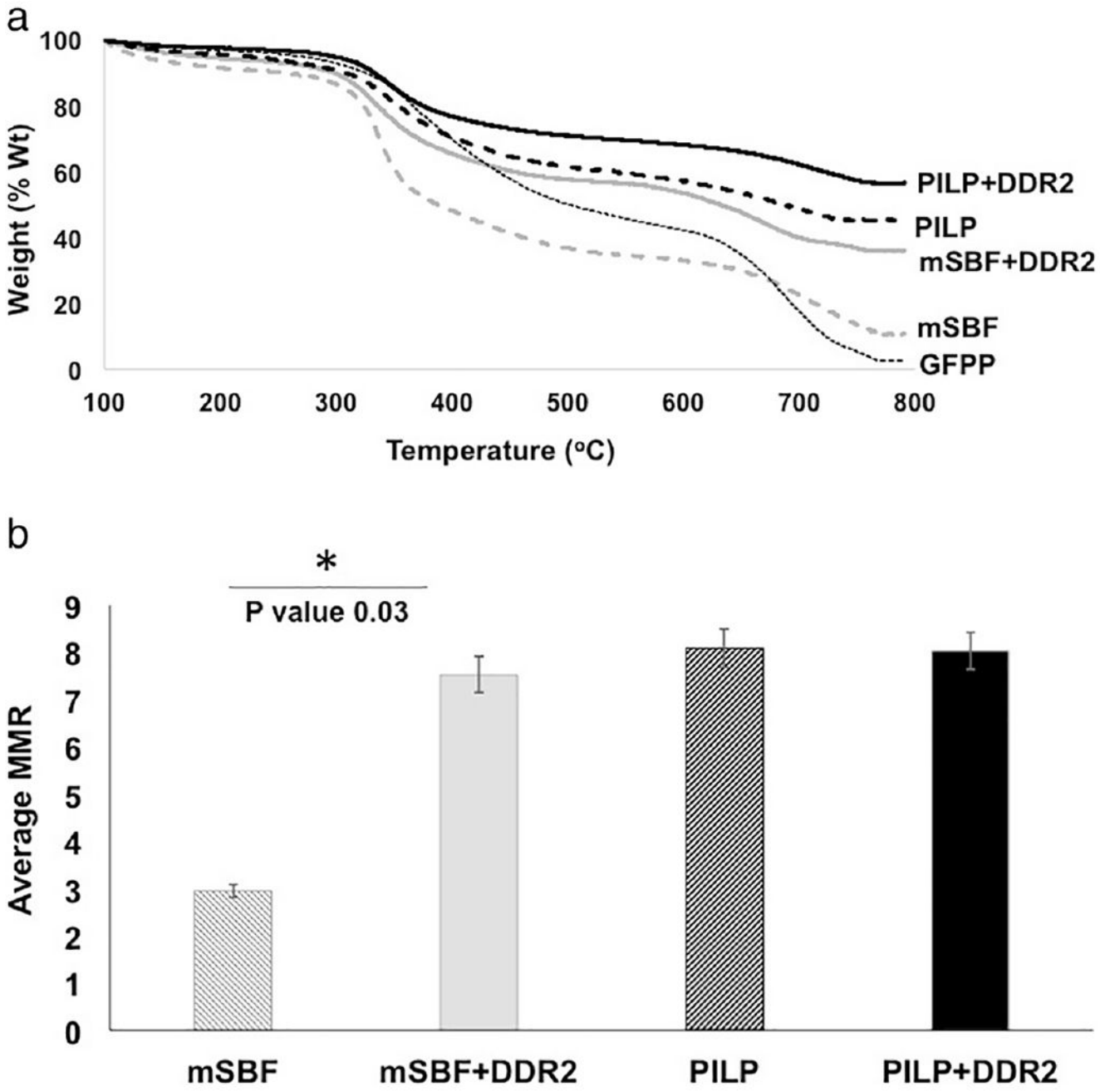

Figure 1:

Analysis of mineral quantity in biomimetically mineralized GFPP using Thermogravimetric Analysis (TGA). (a) Remaining weight percentage after heating the samples up to 800°C and (b) Mineral to matrix ratio (MMR) ascertained from TGA analysis showed significant increase in the presence of DDR2 for mSBF samples (p=0.01) with no significant difference in PILP samples with or without DDR2-Fc (p=0.67).

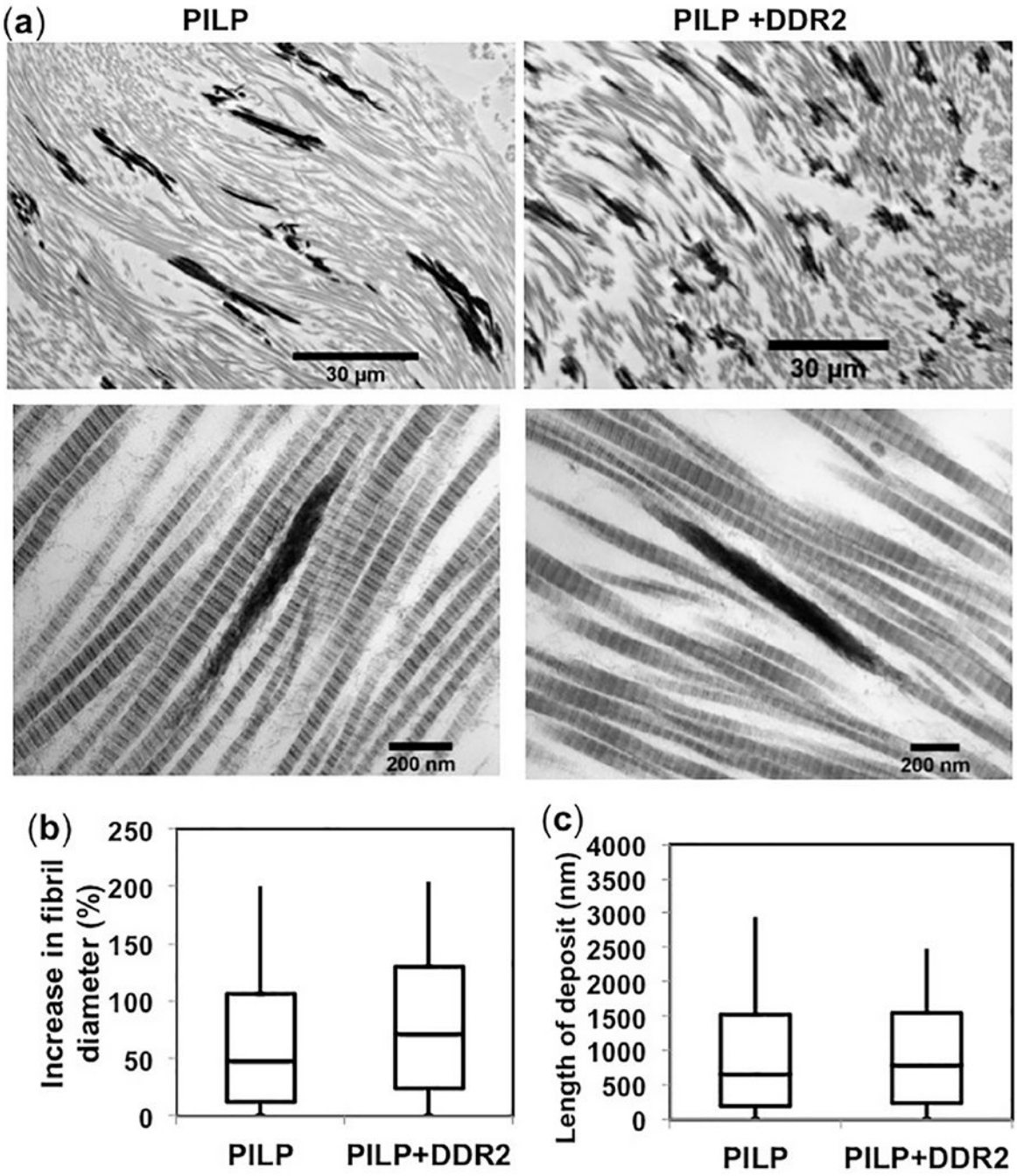

Figure 2:

Micromorphology of mineral deposits in PILP samples. (a) Bright-field TEM micrographs showing intra-fibrillar mineralization as dark, electron-dense deposits, co-linear with collagen fibrils in GFPP subjected to PILP with or without DDR2-Fc as indicated. Quantification of (b) percent increase in fibril diameter and (c) length of intra-fibrillar mineral deposits revealed no significant differences in these parameters between samples with or without DDR2-Fc (p-value>0.05).

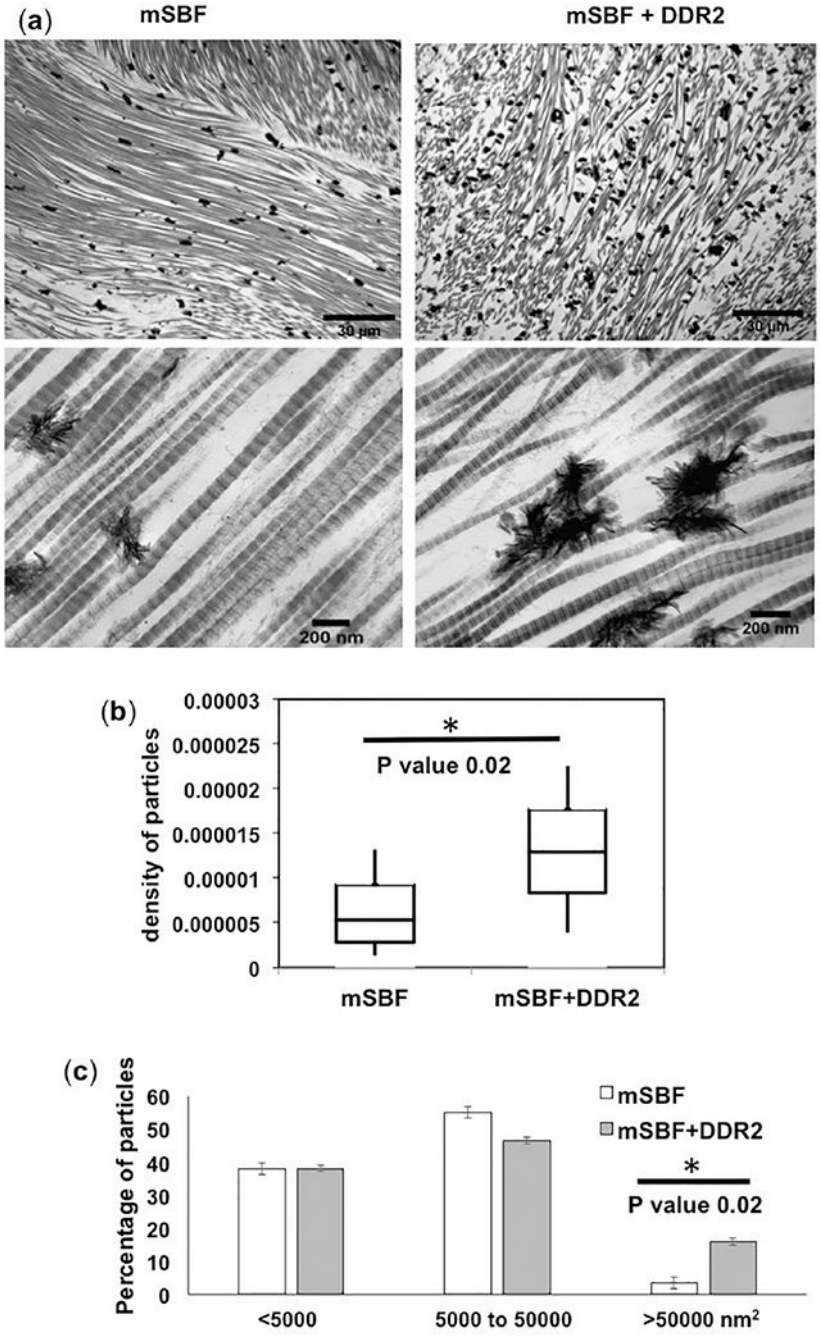

Figure 3:

Micromorphology of mineral deposits in mSBF samples. (a) Bright-field TEM micrographs showing extra-fibrillar mineralization as dark, electron-dense deposits, decorating collagen fibrils in GFPP subjected to mSBF with or without DDR2-Fc as indicated. Quantification of (b) particle density, i.e. number of mineral particles per nm^2 of collagen, and (c) size distribution of extra-fibrillar mineral deposits revealed that samples with DDR2-Fc exhibited a significant increase in particle density ($p=0.02$) and a higher population of particles with size > 50000 nm^2 ($p=0.02$).

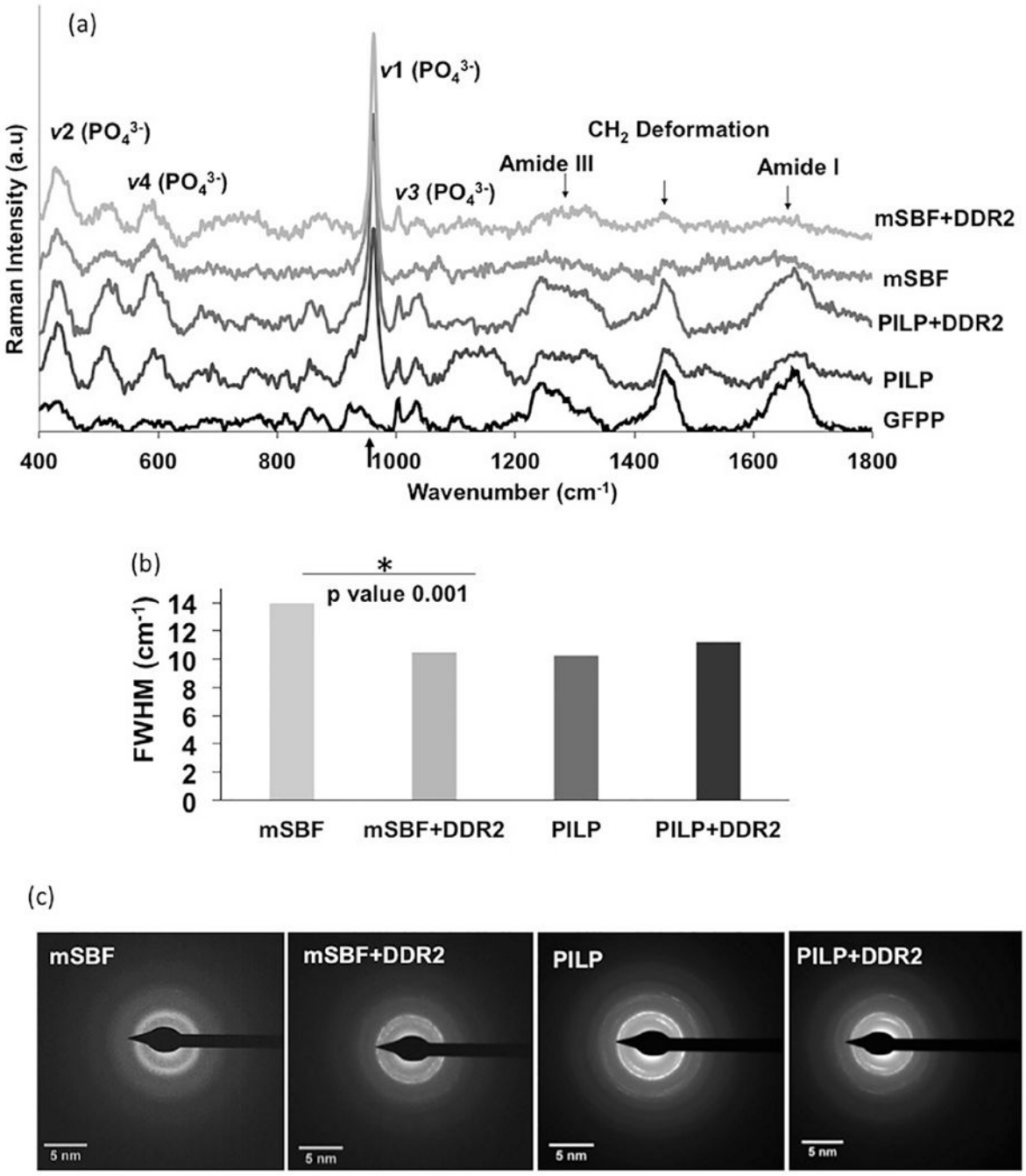

Figure 4:

Raman spectroscopy of GFPP subjected to biomimetic mineralization protocols as indicated. (a) Raman spectra indicating locations of major phosphate and amide bands. (b) Spectral peak width of the major phosphate band at 960 cm^{-1} ascertained using full width at half maximum (FWHM) revealed that DDR2-FC decreased the FWHM in mSBF samples ($p=0.001$) with no significant change in the PILP samples ($p=0.34$). ,(c) Selective area electron diffraction (SAED) patterns from mineral deposits identified in TEM images show diffuse pattern in mSBF samples but presence of discrete rings in all other samples.

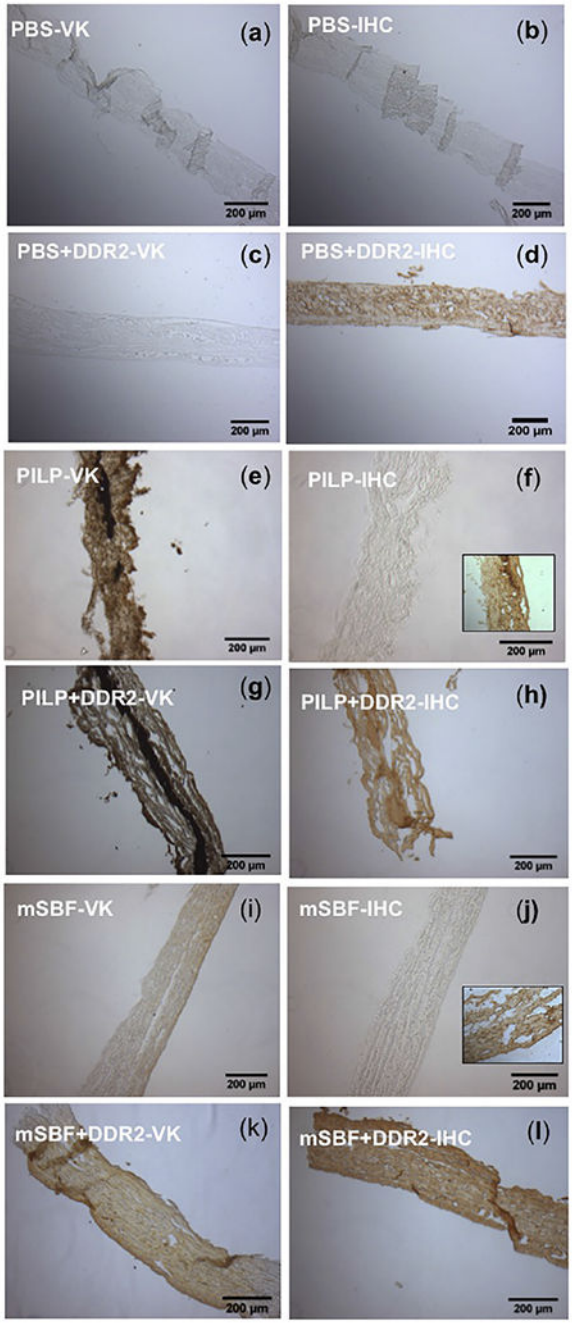

Figure 5:

Histological analysis of GFPP incubated in PBS, PILP and mSBF in the presence or absence of DDR2-Fc as indicated. Brown color indicates presence of Calcium (in Von kossa (VK) and of DDR2-Fc in immunohistochemistry (IHC) using anti-Fc antibodies. Mineralization was present in all samples incubated in PILP (e, g) or mSBF (i, k), but not PBS (a, c). Positive staining for DDR2-FC was observed when GFPP was incubated with DDR2-FC in PBS (d), PILP (g) or mSBF (l). Insets in (f) and (j) show positive staining for DDR2-Fc also when GFPP premineralized in PILP or mSBF was incubated with DDR2-FC.

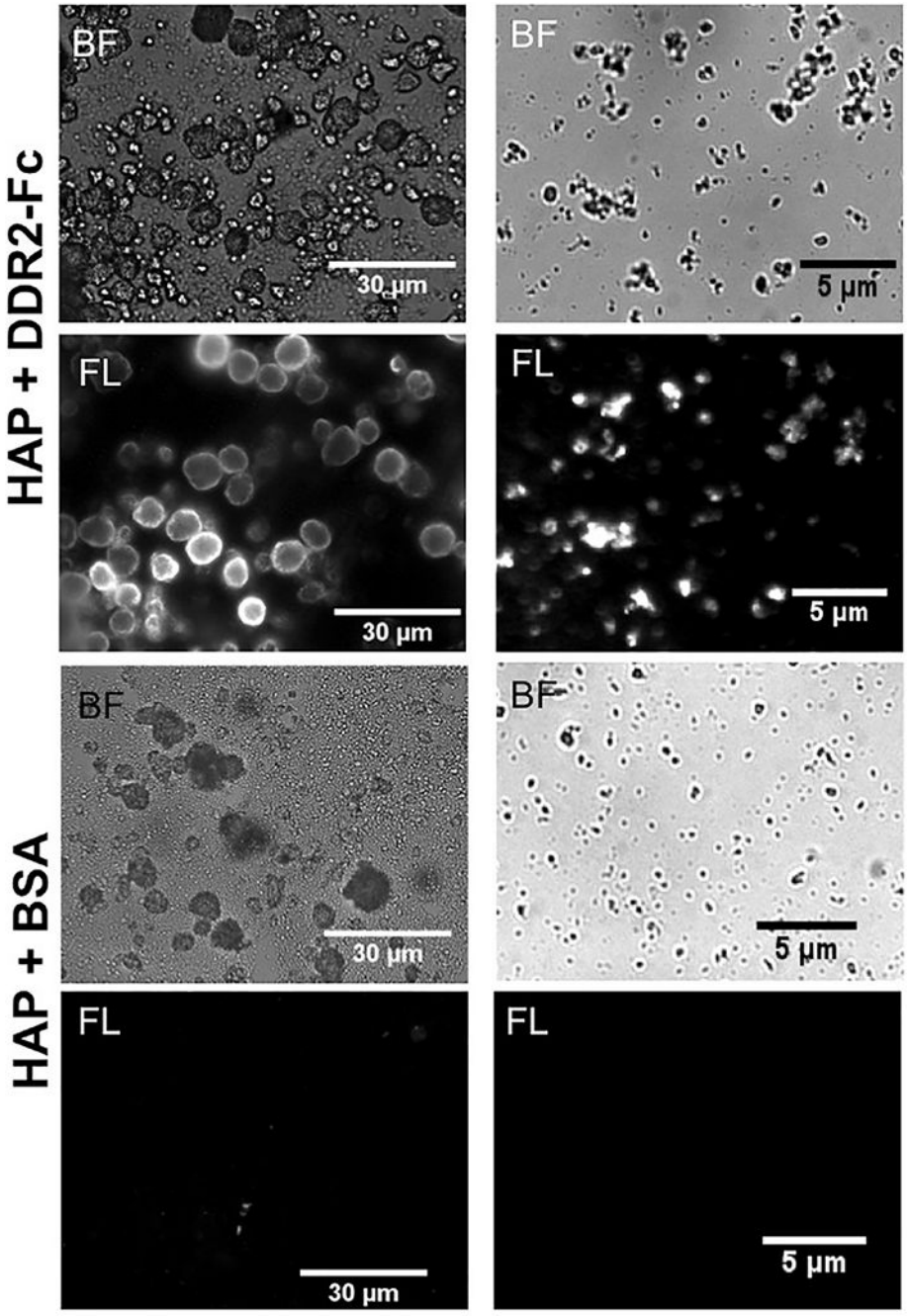

Figure 6:
Immuno-fluorescence (IF) staining (using anti-Fc antibodies) of the HAP particles incubated in 100 μg/ml of DDR2-Fc or BSA as indicated. Bright field (BF) and corresponding fluorescence (FL) images are shown for two representative particle sizes present in the samples. HAP particles incubated with DDR2-Fc showed positive IF signal whereas no non-specific binding of anti-Fc antibody was observed when BSA was used as a control.

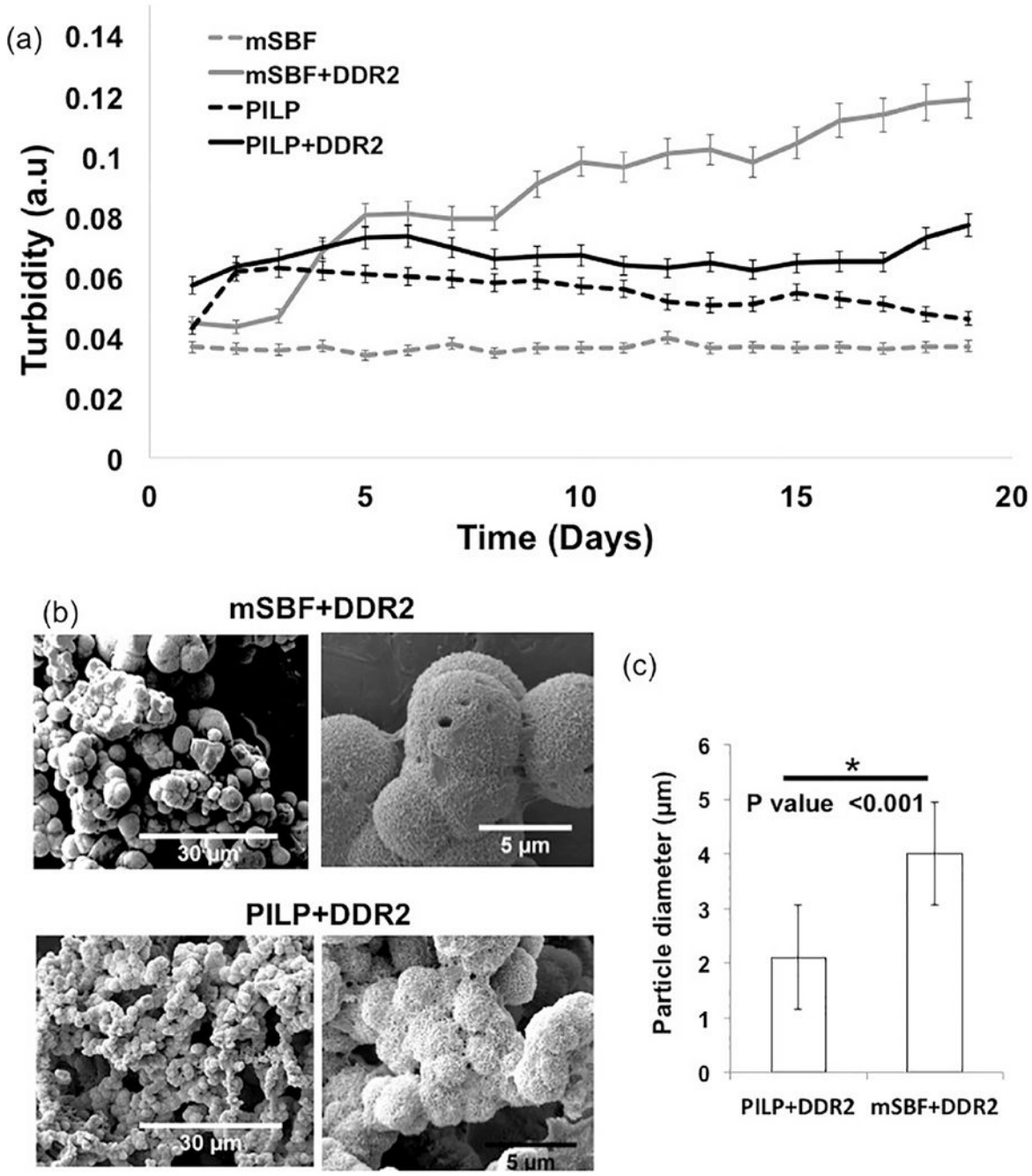

Figure 7:

(a) Absorbance of biomimetic mineralization solutions (containing DDR2-Fc as indicated) up to 21 days, (b) SEM images and (c) particle size analysis of mineral deposits obtained from mSBF and PILP solutions containing DDR2-Fc, showed significantly larger particles in mSBF+DDR2 samples ($p<0.001$).

Table 1:

Reagents used for preparing 1000 ml mSBF

	NaCl	$NaHCO_3$	KCl	$K_2HPO_4 . 3H_2O$	$MgCl_2 \cdot 6H_2O$	$CaCl_2$	Na_2SO_4	Na_2CO_3	HEPES
g/L	5.403	0.504	0.225	0.230	0.311	0.293	0.072	0.426	17.892
mM	100	6	3	1	1.5	2.5	0.5	4	75